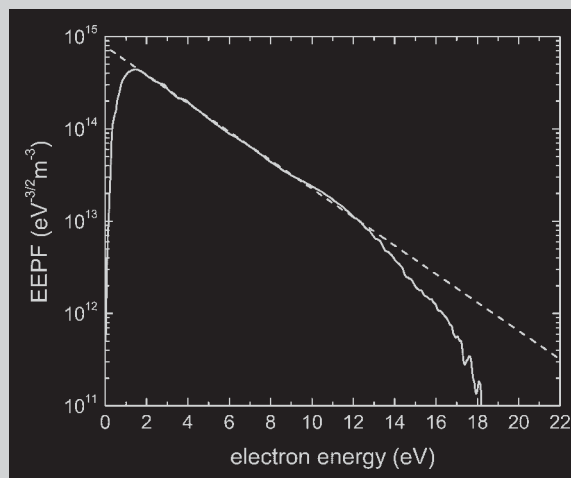


Summary: Electron energy distribution functions (EEDF) are obtained from probe measurement data along the axis of the metallic chamber of an inductively driven tandem plasma source. The numerical procedure for calculating the second derivative of the probe current combines Savitzky-Golay smoothing filter and the three-point differentiator with a varying step. The EEDF is obtained through the Druyvesteyn formula from the calculated second derivative. The shape of the EEDFs in argon gas at low pressures is investigated for the case of a tandem plasma source. Experimental EEDFs are compared with Maxwellian distributions, and deviations in the tail are observed at higher pressures, which are explained in terms of the ratio between the electron-electron collision frequency and the excitation frequency. Axial variations of the slope and of the area below the EEDF curve result in electron temperature and concentration decrease along the axis.



Electron energy distribution function (EEDF) measured for gas pressure of 26 mTorr, at an axial position of 12 cm.

Electron Energy Distribution Function Measurements in an Inductively Driven Tandem Plasma Source

Tsanko Tsankov, Zhivko Kiss'ovski,* Nina Djermanova, Stanimir Kolev

Department of Radiophysics and Electronics, Faculty of Physics, Sofia University, St. Kliment Ohridski, 5 J. Bourchier Blvd., BG-1164 Sofia, Bulgaria
Fax: +359 2 96 25 276; E-mail: kissov@phys.uni-sofia.bg

Received: September 23, 2005; Revised: October 20, 2005; Accepted: October 26, 2005; DOI: 10.1002/ppap.200500092

Keywords: electron-energy distribution function (EEDF); inductively-coupled plasmas; Langmuir electrostatic probe (LEP); plasma sources

Introduction

Inductively coupled plasma sources operating at low gas pressures have been used as ion sources for particle accelerators, and also in plasma processing and lighting sources.^[1] In many applications, plasma produced by a cylindrical inductive discharge is transported to a processing chamber where the substrate is positioned.^[1,2] Plasma parameters in this region are quite different than the parameters in the driver region, and they vary with the axial distance. Their prediction requires modelling^[3] or space resolved measurements in both regions and such results are very scarce in the literature.^[4,5]

Measurements of the EEDF are important for determining the plasma parameters and for optimizing the plasma processes used for various applications.^[1,2,6] The shape of the EEDF significantly affects the effectiveness of ion beam sources, especially in tandem plasma sources used for the production of negative hydrogen ions. In the second chamber of such plasma sources, the plasma density and the electron energy substantially decrease in comparison with those in the driver region, which requires investigation of the spatial variations of the EEDF. Probe diagnostics technique is a commonly used method for determination of EEDF because of its simple design and its good spatial resolution. The EEDF shape in the driver and extraction

regions of the tandem negative ion source is well investigated for filament discharge in hydrogen.^[4,5] The changes of the EEDF in inductive discharges in argon with variations of the neutral gas pressure and applied power are obtained by Godyak et al.^[6] Our measurements of EEDF are performed in a large diameter metallic chamber where the argon plasma (produced in small diameter quartz tube by an inductive discharge) expands, and therefore variations of the plasma parameters with the distance from the discharge are expected. The EEDF is obtained from the Druyvesteyn formula^[7] and the calculations of the second derivative of the current-voltage (I-V) probe characteristics. Different methods have been developed to obtain the second derivative of the probe current: analogue devices,^[6,8] numerical differentiation of the probe characteristics,^[4,9,10] or mixed methods.^[11] Advantage of the numerical processing of the probe data for EEDF determination is the short time of measurements,^[12] which limits the contamination of the probe's surface. The aim of this study is the experimental investigations of the axial variation of the shape of the EEDF in the plasma expansion region of an inductively driven tandem plasma source.

Experimental Part

The experiments were performed in the second chamber of an inductively driven tandem plasma source (Figure 1). The plasma was created in the first chamber of the source, in the driver region. It is a quartz tube with a length of 300 mm and an inner diameter of 45 mm. The plasma produced here expanded in a second metal chamber, the expansion chamber, which was a stainless steel vessel with a length of 470 mm and a diameter of 220 mm. The plasma was sustained by an inductive

discharge with a nine-turn copper coil driven at 27 MHz. The output power of the RF generator was adjusted so that the coil delivers approximately 160 W of HF power to the plasma. The working gas was argon at pressures in the range of 8 to 26 mTorr.

The measurements were performed in the expansion region of the plasma source by an axially movable single Langmuir probe. The probe was a tungsten wire with a length of 4 mm and a diameter of 0.1 mm. To avoid the distortion of the probe characteristic from the HF field, four resonant chokes and a floating electrode were incorporated in the probe head. The chokes were tuned to the fundamental and to the second harmonic frequency of the driving signal of 27 MHz. The I-V characteristic of the probe was measured by an acquisition system.^[12] The system consists of a ramp generator and a high-voltage amplifier, which produced a linear ramp (−70 to +30 V) with a repetition frequency of 160 Hz. The probe current was converted into voltage through a transimpedance amplifier and it was registered by a digital oscilloscope. The waveforms of the probe voltage and probe current were then transferred to a PC for numerical processing.

Numerical methods^[12] were applied to the probe characteristic data in order to obtain the second derivative of the probe current. The procedure included averaging of 2560 characteristics, numerical smoothing and differentiation. For the numerical smoothing a second order Savitzky-Golay filter was used. The three-point differentiator modification with changing differentiation step was used for the calculation of the second derivative of the smoothed probe characteristic. This method allowed additional noise suppression and good energy resolution. The EEDF ($F(E)$, where E is the electron energy) was obtained via the Druyvesteyn formula from the second derivative of the probe current (I_e):

$$F[E = e(U_{pl} - U)] = \frac{\sqrt{8m_e}}{Se^3} \sqrt{E} \frac{d^2 I_e}{dU^2} \quad (1)$$

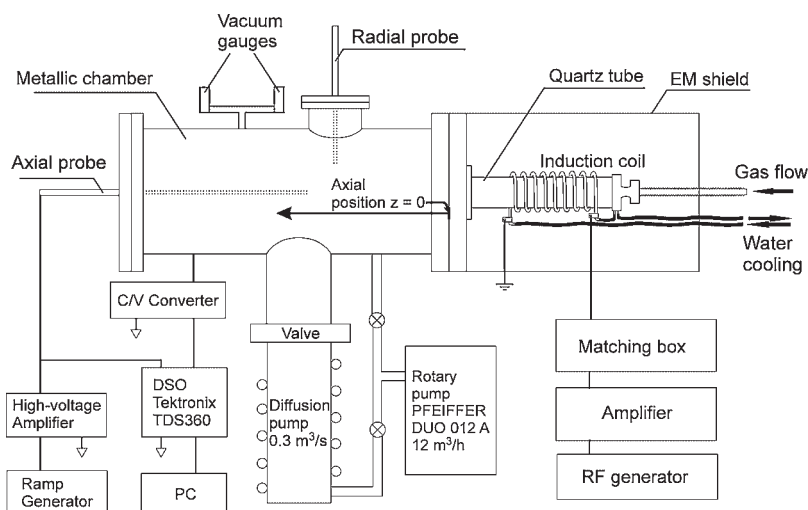


Figure 1. Schematic representation of the experimental set-up and of the probe diagnostic system.

Here m_e , e , S , U_{pl} , and U are the electron mass, charge, probe area, plasma potential and the voltage applied to the probe, respectively. For comparison with a Maxwellian distribution, EEPF ($F_p(E) = F(E)/\sqrt{E}$) instead EEDF was used. The plasma density, n_e , and the temperature, T_e , corresponding to the mean electron energy were also obtained by numerical integration of the EEDF:

$$n_e = \int_0^{E_{\max}} F(E) dE \quad (2)$$

$$T_e = \frac{2}{3kn_e} \int_0^{E_{\max}} E F(E) dE \quad (3)$$

where k is the Boltzmann constant and E_{\max} is the energy for which the second derivative of the ion current is comparable with that of the electron current.

Results and Discussion

The EEPFs measured for distances $z = 2, 6, 12$ and 22 cm from the end of driver region ($z = 0$), are presented in Figure 2 and 3 for pressures $p = 8$ and 26 mTorr, respectively. The Maxwellian distribution is presented by

dashed lines in the figures. The results show that at lower pressure (8 mTorr) the EEPF is Maxwellian for all axial positions. The body of the EEPF at $p = 26$ mTorr has a Maxwellian shape while the tail deviates from Maxwellian in the inelastic energy range ($E > E^*$). The electron temperature obtained from the slope of the measured EEPF bodies decreases with the distance from the driver region from 3 eV at $z = 2$ cm to 2.6 eV at $z = 22$ cm for $p = 8$ mTorr, and from 2.9 eV at $z = 2$ cm to 2.5 eV at $z = 22$ cm at $p = 26$ mTorr. The electron density decreases along the axis from $1.7 \times 10^{16} \text{ m}^{-3}$ to $0.64 \times 10^{16} \text{ m}^{-3}$ at $p = 8$ mTorr, and from $3.0 \times 10^{16} \text{ m}^{-3}$ to $0.32 \times 10^{16} \text{ m}^{-3}$ for $p = 26$ mTorr, for the same axial positions. The body of the EEDFs is Maxwellian for both pressures at all axial positions because the electron-electron collision frequency ν_{ee} is higher than $2m_e\nu_{en}/M_i$, which is the characteristic frequency for energy transfer in electron-neutral elastic collisions (ν_{en} is the electron-neutral collision frequency and M_i is the neutral mass).^[3] In the investigated pressure range, and with the obtained values of the electron temperatures, the value of the excitation frequency ν^* is higher than the ionization frequency ν^i .^[1,6] The $\nu^*(T_e)$ dependence is presented by continuous and dashed curves in Figure 4 for $p = 8$ mTorr and $p = 26$ mTorr, respectively.

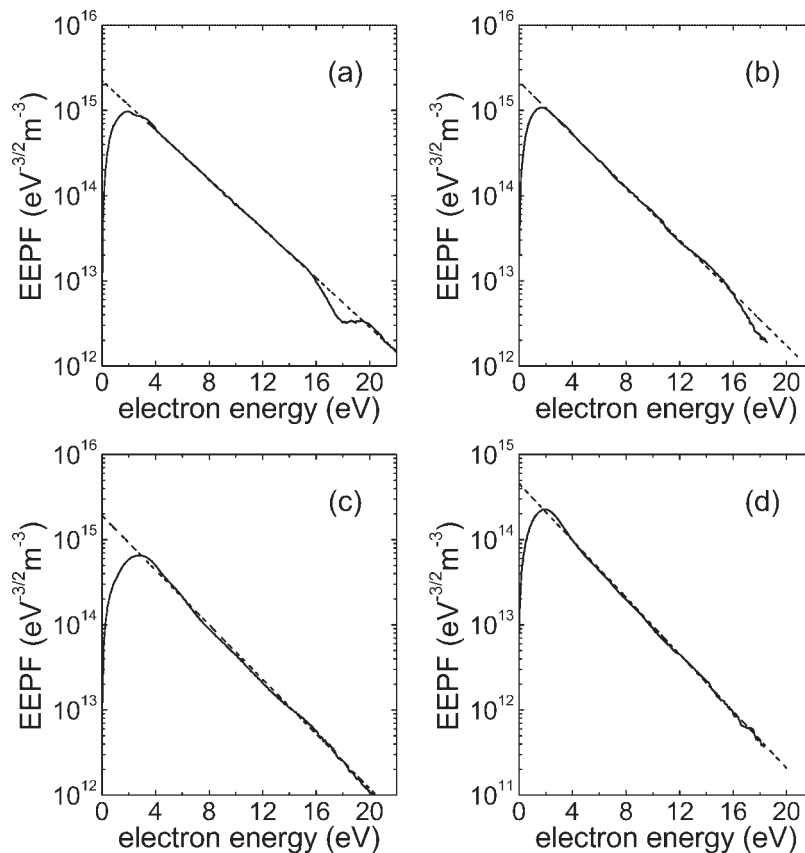


Figure 2. EEPFs measured at $p = 8$ mTorr for different axial positions: (a) $z = 2$ cm, (b) $z = 6$ cm, (c) $z = 12$ cm, (d) $z = 22$ cm.

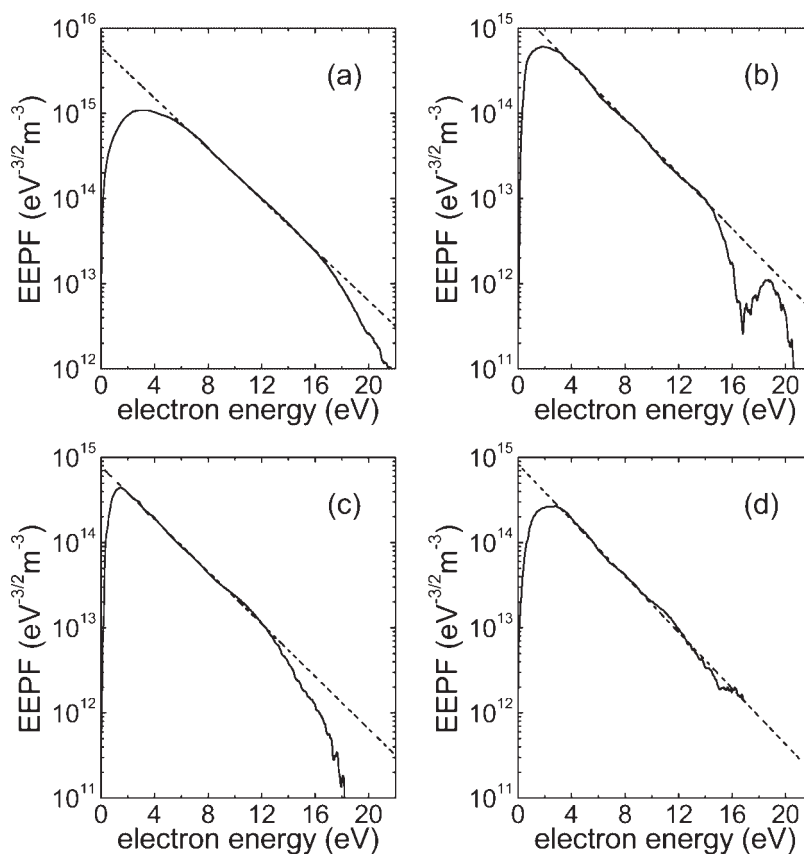


Figure 3. EEPFs measured at $p = 26$ mTorr for different axial positions: (a) $z = 2$ cm, (b) $z = 6$ cm, (c) $z = 12$ cm, (d) $z = 22$ cm.

The electron-electron collision frequency decreases along the axis due to fast decrease of the electron concentration regardless of the decrease of the electron temperature. The result shows that the experimentally obtained values (solid points) of the collision frequency ν_{ee}

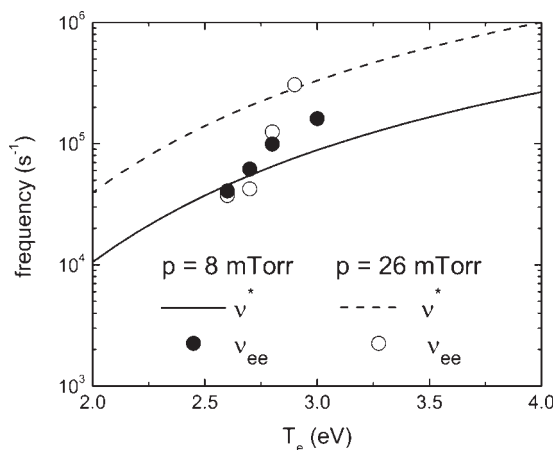


Figure 4. Comparison of the electron-electron collision frequency, ν_{ee} at $z = 2, 6, 12, 22$ cm and the excitation frequency $\nu^*(T_e)$ for pressures $p = 8$ mTorr and $p = 26$ mTorr.

are higher than the excitation frequency ν^* (solid curve) at $p = 8$ mTorr. This ensures the Maxwellian shape of the EEDF. The values of ν_{ee} (open circles) along the axis at 26 mTorr are lower than ν^* (dashed curve) and, consequently, the shape of the EEDFs deviates from a Maxwellian one in the inelastic energy range.

The electron temperatures at $z = 6$ cm are $T_e = 2.8$ eV (for $p = 8$ mTorr) and $T_e = 2.7$ eV (for $p = 26$ mTorr). The results we obtained show that after a faster drop close to the end of the driver region, reported also in another work,^[13] the electron temperature decreases slowly with the distance. The energy relaxation length $\lambda_E = \lambda_{en} / \sqrt{2m_e/M_i}$ in the elastic energy region is larger than the metal chamber length which explains the weak changes of electron temperature along the axis for $z > 6$ cm (λ_{en} is the electron mean free path for elastic collisions with neutrals).

The deviation of the EEDF from Maxwellian distribution depends on the ratio of the excitation frequency to the electron-electron collision frequency at every axial position. At intermediate pressure in the investigated pressure range, the change of the EEDF tail (non-Maxwellian to Maxwellian) is expected because the decrease of the plasma density with the axial distance from the end of the driver region.

Conclusion

Electron energy distribution functions in the expansion chamber of a tandem plasma source are obtained for different axial positions. In argon gas at pressure $p = 8$ mTorr, the EEDFs we obtained are Maxwellian for all axial positions z ($z = 2$ cm to 22 cm). The body of the EEDFs for $p = 26$ mTorr has a Maxwellian shape, while the tail deviates from the Maxwellian one in the inelastic energy range because the electron-electron collision frequency is lower than the excitation frequency. For $z \geq 6$ cm, the electron temperature decreases slowly with the distance due to a large energy relaxation length in comparison with the chamber length.

Acknowledgements: This work is within EURATOM-project FU06-CT-2003-00139 and project no. 1316 supported by the Ministry of the Education and Science in Bulgaria.

- [1] "Advanced Technologies Based on Wave and Beam Generated Plasmas", H. Schlüter, A. Shivarova, Eds., Kluwer, Dordrecht 1998.
- [2] J. Hopwood, *Plasma Sources Sci. Technol.* **1992**, *1*, 109.
- [3] H. J. Yoon, C. Charles, R. W. Boswell, *J. Phys. D: Appl. Phys.* **2005**, *38*, 2825.
- [4] M. B. Hopkins, M. Bacal, W. G. Graham, *J. Phys. D: Appl. Phys.* **1991**, *24*, 268.
- [5] M. B. Hopkins, W. G. Graham, *Vacuum* **1986**, *36*, 873.
- [6] V. A. Godyak, R. B. Piejak, B. M. Alexandrovich, *Plasma Sources Sci. Technol.* **2002**, *11*, 525.
- [7] M. J. Druyvesteyn *Z. Phys.* **1930**, *64*, 790.
- [8] H. Amemiya, *J. Phys. D: Appl. Phys.* **1990**, *23*, 999.
- [9] F. Fujita, H. Yamazaki, *Jpn. J. Appl. Phys.* **1990**, *29*, 2139.
- [10] E. Tatarova, F. M. Dias, *J. Phys. IV* **1998**, *8*, 257.
- [11] F. M. Dias, *Plasma Sources Sci. Technol.* **1995**, *4*, 86.
- [12] N. Djermanova, Zh. Kiss'ovski, Ts. Tsankov, *Contrib. Plasma Phys.*, accepted for publication.
- [13] M. Dimitrova, N. Djermanova, Zh. Kiss'ovski, St. Kolev, A. Shivarova, Ts. Tsankov, *Plasma Process. Polym.* **2006**, *3*, 156.